Robust Stabilization of Axial Flow Compressor Dynamics Via Sliding Mode Design

Der-Cherng Liaw
Department of Electrical and Control Engineering,
National Chiao Tung University,
Hsinchu, 30010 Taiwan, Republic of China
e-mail: dcliaw@cc.nctu.edu.tw

Jeng-Tze Huang
Department of Electronic Engineering,
Van Nung Institute of Technology,
Chungli, 340 Taiwan, Republic of China
e-mail: jthuang@cc.vit.edu.tw

Issues of the robust stabilization for axial-flow compressor dynamics with respect to the uncertainty in axisymmetric characteristics are presented. This is achieved by the design of sliding mode controllers. By assuming an actuation directly modulating the mass flow such as the close-coupled valve, the domain of attraction for the unstalled operating equilibrium will be enlarged to a great extent. Nonlocal robust stability of the operating equilibrium, with respect to the uncertainty in the unstable branch of axisymmetric compressor characteristic, is also provided by the proposed control laws. Moreover, it is demonstrated that the robust control scheme can be employed to fulfill the task of stall recovery. The proposed stabilization design does not require an explicit form for compressor characteristic. [DOI: 10.1115/1.1386393]

1 Introduction

Axial flow compressors are widely used in both aerospace and industrial applications due to their potential of high efficiency. To achieve high efficient operation of an engine, the air prior to combustion is known to be greatly compressed by compressor [1]. However, when a compressor operates close to its maximum pressure-rise, two aerodynamic instabilities can happen, both of which reduce system's performance. One is the so-called ''rotating stall,'' which is a dynamic instability that occurs when an asymmetric flow pattern develops in the blade passages of a compressor stage. The other is a large-amplitude, axisymmetric oscillation in the overall pumping system and is known as ''surge behavior.'' The rotating stall will result in a drastic pressure drop of the fluid within the compressor, while surge behavior renders the compressor suffering violent periodic impingements and damages the compressor eventually. Therefore, the prevention of these two instabilities becomes an important issue.

Conventionally, a stall (or surge) line is drawn to provide a safe operation boundary for compressors. Such a conservative tradeoff unduly restricts engine's capability. Therefore, various control schemes have been recently proposed to allow compressors to operate safely beyond the stall line and thus increase system efficiency. Among these, the active control [2] and the bifurcation control [3] designs guarantee local stabilities, while the backstepping designs [4] achieve global stabilities for specific cubic-type compressors. However, the robustness issues and study of noncubic characteristic systems haven't been considered yet.

When there is no 2D distributive actuation available, the compression system described by a three-state model [5] is known to be uncontrollable [3,6,7]. For compressors with the so-called ''left-tilt'' property operating at the stable unstalled equilibrium, the system can be characterized as a nonlinear minimum-phase system [8]. The domain of attraction (DOA) of the unstalled equilibrium has been effectively enlarged by [8]. But, robustness was not considered in that study. It is known that the unstable portion of the compressor axisymmetric characteristic is hard to measure and the associated system uncertainties are inevitable in real applications [9]. A robust control scheme was recently proposed to deal with such uncertainties by assuming the axisymmetric characteristic of a compressor is a specific cubic function [10]. The robust study for compressor systems with noncubic characteristics still haven't been considered.

The major goal of this paper is to study nonlocal stabilization of the unstalled equilibria for ''left-tilt'' type of system subject to uncertainties in the compressor characteristics. This will be achieved by the design of a sliding mode controller. Sliding mode design is characterized by its robustness and low computational requirements [11]. Based on a simplified two-state dynamical model, sliding mode control has been applied to the robust control of surge behavior in compressors [12]. However, the results for stall dynamics had not been obtained yet. There are two main objectives of this paper. One is to attain nonlocal stabilization of the unstalled system equilibria, and the other is to provide systems robustness with respect to the uncertainty in the compressor characteristic. These results will not rely on the explicit forms for the compressor characteristics. The actuation proposed to be utilized in the study is an additive-type control for the mass flow dynamics, which can be practically implemented in several ways [13].

The paper is organized as follows. Section 2 recalls the compression system model developed by [5]. A brief description of compressor dynamics is also given to highlight the motivation of the paper. It is followed by the nonlocal stabilization design of the unstalled equilibria via sliding mode control schemes. The cubic compressor model is adopted in Section 4 to demonstrate the validity of the designs. Finally, conclusions are given in Section 5.

2 Dynamical Equations for Axial Flow Compression Systems

Conceptually, a compression system can be represented by a series of components: inlet duct, compressor, exit duct, plenum and throttle as depicted in Fig. 1. A lumped-parameter model of axial flow compressors introduced by [5] in terms of nondimensional variables using the notation of [3] is recalled as follows:

$$\frac{dA}{dt} = \frac{\alpha}{\pi W}\int_0^{2\pi} C_{ss}(\dot{m}_C + WA\sin\theta)\sin\theta\, d\theta, \tag{1}$$

$$\frac{d\dot{m}_C}{dt} = -\Delta P + \frac{1}{2\pi}\int_0^{2\pi} C_{ss}(\dot{m}_C + WA\sin\theta)\, d\theta, \tag{2}$$

$$\frac{d\Delta P}{dt} = \frac{1}{4B^2}\{\dot{m}_C - F(\gamma, \Delta P)\}. \tag{3}$$

Contributed by the Dynamic Systems and Control Division for publication in the JOURNAL OF DYNAMIC SYSTEMS, MEASUREMENT, AND CONTROL. Manuscript received by the Dynamic Systems and Control Division July 28, 1998. Associate Editor: A. Sinha.

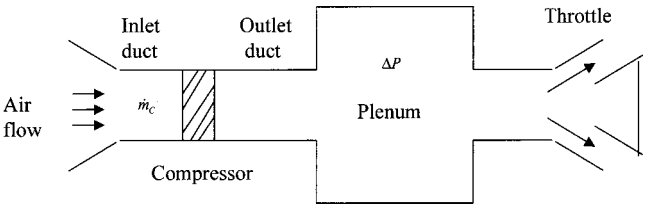

Fig. 1 Schematic diagram of an axial-flow compression system

The quantities appearing in the model above are given in the Nomenclature. In the dynamical equations above, Eq. (2) is obtained from momentum balance and implies that the acceleration of the fluid in the inlet and outlet ducts is proportional to the difference between the pressure rise across the compressor and that in the plenum. The variable of integration θ represents the angular displacement from a reference stationary with the first harmonic mode of the stall wave [5]. Moreover, Eq. (1) determines the rate of amplitude $A(t)$, while Eq. (3) governs the change rate of the plenum pressure. The compressor axisymmetric characteristic $C_{ss}(\cdot)$, characterizing the steady pressure rise across the compressor, is often an S-shaped function and can be modeled by a suitable nonlinear function [5]. It is observed that the nonlinearities of system (1)–(3) mainly come from the axisymmetric compressor characteristic $C_{ss}(\cdot)$ and the throttle characteristic function $F(\gamma,\Delta P)$. In this paper, $C_{ss}(\cdot)$ is assumed to be smooth enough while $F(\gamma,\Delta P)$ is assumed to be strictly increasing with respect to both γ and ΔP.

Normally, the system (1)–(3) operates at the stable unstalled equilibrium of which $A=0$. Denote $x^0=(0,\dot{m}_C^0,\Delta P^0)^T$ an unstalled equilibrium point. By letting $A=0$, it is easy to check from Eqs. (2)–(3) that $\dot{m}_C^0=F(\gamma_0,\Delta P^0)$ and $\Delta P^0=C_{ss}(\dot{m}_C^0)$ for given $\gamma=\gamma_0$. In addition, there usually exists another equilibrium branch for system (1)–(3) with $A\neq 0$, which is the so-called ''stalled equilibria.'' The nominal unstalled operating point are known to be locally asymptotically stable (resp. unstable) for $C'_{ss}(\dot{m}_C^0)<0$ (resp. for $C'_{ss}(\dot{m}_C^0)>0$) [3]. Moreover, the unstalled operating points are found to lose linear stability at the point with $C'_{ss}(\dot{m}_C^0)=0$. This operating point is the so-called ''stall inception point'' at which both stalled and unstalled system equilibria join together due to the occurrence of stationary bifurcation [3]. When compressor operates at an unstalled point near the stall inception point, a small perturbation of the throttle control value or large enough disturbance might cause the compression system to exhibit a jumping behavior from stable operation to some other stable stalled equilibrium due to the coexistence of multiple equilibria. This results in a sudden drop of the pressure rise and the occurrence of rotating stall in real operations.

For illustrations, typical time responses and bifurcation diagrams for a compressor with cubic characteristic defined in Eq. (22) of Section 4 are depicted in Figs. 2 and 3. In Figs. 2(*d*) and 3(*d*), solid curves denote stable equilibria while dotted curves represent unstable equilibria with respect to the variation of throttle setting. The system equilibria are plotted in $\Delta P-\dot{m}_C$ plane, which are obtained by solving Eqs. (1)–(3) via the code AUTO [14]. Denote γ_s and γ_c, respectively, the values of γ at which the compression system exhibits saddle-node bifurcation and stationary bifurcation [15]. The throttle control functions for $\gamma=\gamma_s$ and $\gamma=\gamma_c$ are shown in Figs. 2(*d*) and 3(*d*) as two dash-dotted lines. It is clear from the discussions above that the throttle function for $\gamma=\gamma_c$ intersects the axisymmetric compressor characteristic $C_{ss}(\dot{m}_C)$ at the point $\dot{m}_C=\dot{m}_C^P$ with $C'_{ss}(\dot{m}_C^P)=0$, i.e., the local peak point of $C_{ss}(\dot{m}_C)$ as depicted in Figs. 2(*d*) and 3(*d*). Since $C'_{ss}(\dot{m}_C)<0$ for $\dot{m}_C>\dot{m}_C^P$, the unstalled operating equilibrium $x^0=(0,\dot{m}_C^0,\Delta P^0)^T$ is hence stable for $\dot{m}_C^0>\dot{m}_C^P$. On the contrary, $C'_{ss}(\dot{m}_C)>0$ for $1<\dot{m}_C<\dot{m}_C^P$. Thus, the unstalled operating equilibrium x^0 is unstable for $1<\dot{m}_C^0<\dot{m}_C^P$. The other curve, which emerges from the local peak point of $C_{ss}(\dot{m}_C)$ and is plotted by dotted-line connecting with solid-line, denotes the equilibrium solution of (1)–(3) with $A\neq 0$. This solution curve is marked as ''stalled equilibria'' as depicted in Fig. 2(*d*).

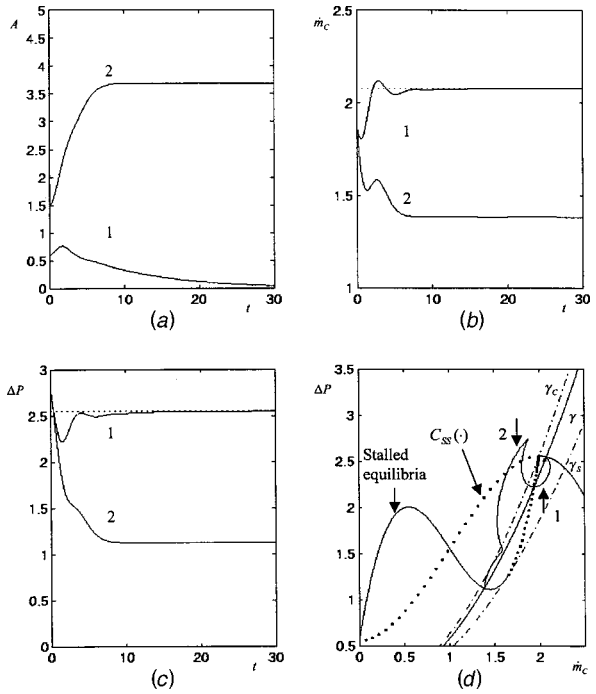

Fig. 2 Jump behavior for operation in the prestalled zone (*a*) A versus t, (*b*) mass flow versus t, (*c*) pressure rise versus t, (*d*) plot in the phase plane

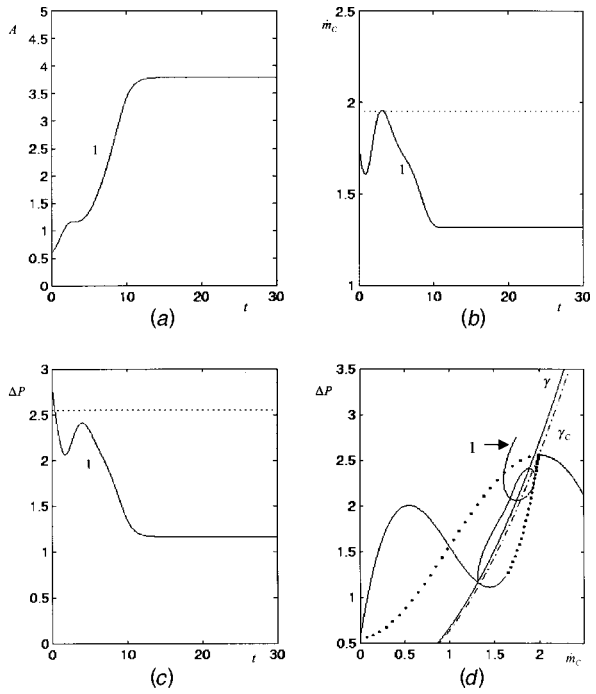

Fig. 3 Jump behavior for operation in the stalled zone (*a*) A versus t, (*b*) mass flow versus t, (*c*) pressure rise versus t, (*d*) plot in the phase plane

Multiple system equilibria are observed to coexist for $\gamma \leqslant \gamma_s$. For instance, consider the time response for the case of which $\gamma_c < \gamma < \gamma_s$ as depicted in Figs. 2(*a*)–2(*d*). The two transient trajectories denoted as 1 and 2 in Fig. 2(*d*) go to different final states for the same value of the throttle control value. Initial states of trajectories 1 and 2 are, respectively, given by $x_{01} = [0.6, 1.88, 2.769]^T$ and $x_{02} = [1.5, 1.88, 2.769]^T$. The jumping behavior associated with trajectory 2 is obviously caused by a large disturbance of the initial condition, which makes the system state eventually settles down to an equilibrium with a finite amplitude of stall wave and a much lower pressure rise as depicted in Figs. 2(*a*)–2(*d*). For smaller disturbance, the system state marked as trajectory 1 returns back to the original unstalled equilibrium as depicted in Figs. 2(*a*)–2(*d*). The jumping behavior, as presented above, might also attribute to a perturbation of the throttle control value as depicted in Fig. 3. In Figs. 3(*a*)–3(*d*), the system state with initial x_{01} jumps to a stable stalled equilibrium along trajectory 1 for the perturbed control value $\gamma < \gamma_c$.

By intuition, the rotating stall occurring for $\gamma_c < \gamma \leqslant \gamma_s$ due to finite-size disturbance might be avoided by making the DOA of the unstalled equilibrium large enough. However, suitable stall recovery schemes are required to be undertaken for annihilating rotating stall for $\gamma < \gamma_c$ [16]. One of commonly used stall recovery control schemes is to push the system response toward a stable unstalled equilibrium by setting a new value of the throttle control parameter γ to assure $\gamma > \gamma_c$ and to make the difference $\gamma - \gamma_c$ large enough. But, such control scheme apparently decreases the efficiency of engine. It is obvious that the efficiency loss by such a stall recovery scheme will be minimized if the DOA of the desired unstalled equilibrium can be effectively enlarged. A sliding mode control scheme is proposed in the next section to fulfill these two tasks with respect to the uncertainty in the compressor characteristics.

3 Robust Stabilization

Though it is known that the compression system is uncontrollable under throttle control input [3,6,7], the throttle control has been used to stabilize the bifurcated solution branch [3,4] or to fulfill the task of the stall recovery [16]. In order to study the robust stabilization of system (1)–(3), the compression system is assumed to have one more control input available. Denote $x^0 = (0, \dot{m}_C^0, \Delta P^0)^T$ the desired unstalled equilibrium at some $\gamma = \gamma^0$. Let $x = (x_1, x_2, x_3)^T$ with $x_1 = A$, $x_2 = \dot{m}_C - \dot{m}_C^0$, $x_3 = \Delta P - \Delta P^0$, and $u_2 = \gamma - \gamma^0$ be the throttle control force. System (1)–(3) can then be rewritten as

$$\frac{dx_1}{dt} = \frac{\alpha}{\pi W} \int_0^{2\pi} C_{ss}(x_2 + \dot{m}_C^0 + W x_1 \sin\theta) \sin\theta \, d\theta \tag{4}$$

$$\frac{dx_2}{dt} = -x_3 - \Delta P^0 + \frac{1}{2\pi} \int_0^{2\pi} C_{ss}(x_2 + \dot{m}_C^0 + W x_1 \sin\theta) \, d\theta + u_1(t) \tag{5}$$

$$\frac{dx_3}{dt} = \frac{1}{4B^2} \{ x_2 + \dot{m}_C^0 - F(\gamma^0 + u_2(t), x_3 + \Delta P^0) \}. \tag{6}$$

Here, $u_1(t)$ is an additive-type control input assumed to be available in the control design. Implementation of such control is not hard to find. For instance, the close-coupled valve is one of choices [12] and another ways of implementation can be found in [13].

It is easy to check that system (4)–(6) is uncontrollable since $A = 0$ is an invariant manifold. According to [3], that means no linear control laws can be obtained by u_1 and u_2 to provide the stability of the unstalled operating equilibrium which is near the stall inception point and lies on the unstable equilibrium branch of the uncontrolled model. In this paper, we will focus on the design for fulfilling two main objectives. One is to enlarge the domain of attraction for the stable unstalled operating equilibrium point x^0, and the other is to provide a scheme for stall recovery when rotating stall occurs at $\gamma < \gamma_c$. The design is shown in Section 3.2 to be robust with respect to the uncertainty of the $C_{ss}(\cdot)$ function. Details are given as follows.

3.1 Uncertainty in the Axisymmetric Characteristic $C_{ss}(\cdot)$. It is known that the stable portion of the C_{ss} function can usually be determined by careful experiment. On the contrary, the unstable branch can hardly be measured. The uncertainty in system dynamics is hence inevitable. From the structure of system dynamics (4)–(6), such kind of uncertainty belongs to the so-called ''mismatched'' type and is not easy to manipulate using traditional methodologies. Nevertheless, based on the four assumptions (H1)-(H4) given in Hypothesis 1, a sliding mode control scheme can still be employed to achieve robust, nonlocal asymptotic stability for the unstalled operating point subjecting to such ''mismatched-type'' uncertainty. Detailed are given as follows.

First, we recall the definition of concave function as given in the following.

Definition 1. A real-valued function ϕ is said to be concave on interval $J \subseteq R$ if

$$\phi(x+\eta) - \phi(x) \leqslant \phi'(x) \cdot \eta \quad \text{for all} \quad x \in J \quad \text{and} \quad x + \eta \in J. \tag{7}$$

To facilitate the stabilization design, we make the following hypothesis.

Hypothesis 1. Suppose the axisymmetric compressor characteristic $C_{ss}(\cdot)$ satisfies the following conditions:

(H1) $C_{ss}(\dot{m}_C)$ is a C^2 function with a local maximum $C_{ss}(\dot{m}_C^P) > 0$ at $\dot{m}_C = \dot{m}_C^P$.

(H2) $C_{ss}(\dot{m}_C)$ is strictly decreasing with $C_{ss}''(\dot{m}_C) \leqslant 0$ for all $\dot{m}_C \geqslant \dot{m}_C^P$.

(H3) $C_{ss}(\dot{m}_C) > 0$ for all $\dot{m}_C < \dot{m}_C^P$.

(H4) $C_{ss}(\dot{m}_C)$ satisfies the so-called ''left-tilt'' property [8], i.e., $C_{ss}(\dot{m}_C^P + \eta) < C_{ss}(\dot{m}_C^P - \eta)$ for all $\eta > 0$.

According to Definition 1, the compressor characteristic $C_{ss}(\dot{m}_C)$ is a concave function for $\dot{m}_C \geqslant \dot{m}_C^P$ if conditions (H1) and (H2) hold. It is also observed from (H1)-(H2) that there exists a point $\underline{\dot{m}}_C > \dot{m}_C^P$ such that $C_{ss}(\underline{\dot{m}}_C) = 0$. This implies that $C_{ss}(\dot{m}_C) \geqslant 0$ for $\dot{m}_C \leqslant \underline{\dot{m}}_C$ and $C_{ss}(\dot{m}_C) < 0$ for $\dot{m}_C > \underline{\dot{m}}_C$. In practical application, it is reasonable to assume that the unstalled operating point $x^0 = [0, \dot{m}_C^0, \Delta P^0]^T$ satisfies the relation: $\dot{m}_C^P < \dot{m}_C^0 < \underline{\dot{m}}_C$ since $C_{ss}(\dot{m}_C^0) > 0$.

Next result is recalled from [8].

Lemma 1. Suppose Hypothesis 1 holds and $\dot{m}_C^0 + x_2 > \dot{m}_C^P$. Then for system (4)–(6), $x_1 \dot{x}_1 \leqslant 0$ and the equality holds only when $x_1 = 0$.

Remark 1. Compressors satisfying all the conditions of (H1)-(H4) may not be common, but are not rare either [8].

Let the curve L_r denote the right portion of the axisymmetric compressor characteristic $C_{ss}(\dot{m}_C)$ for $\dot{m}_C > \dot{m}_C^P$, which is usually obtainable by careful experiment. As depicted in Fig. 4, the curve denoted by L_{bl} is obtained from the symmetry of the curve L_r with respect to the line $\dot{m}_C = \dot{m}_C^P$. For the robust design, in this paper, the axisymmetric compressor characteristic is assumed to satisfy Hypothesis 1. This implies that the unstable branch of $C_{ss}(\dot{m}_C)$, i.e., the left portion of $C_{ss}(\dot{m}_C)$ for $\dot{m}_C < \dot{m}_C^P$ as marked by dotted-curve, must lie within the shaded region as shown in Fig. 4.

3.2 Sliding Mode Designs. To achieve the main goals of the paper as stated in Section 2, in this subsection, we employ the sliding mode control (SMC) technique to fulfill the design task. In general, SMC design procedure consists of three major steps (see e.g. [17,18]). The first step is to choose a sliding surface, which is a function of system state. It is followed by the design of the controller for governing the motion on the sliding surface such

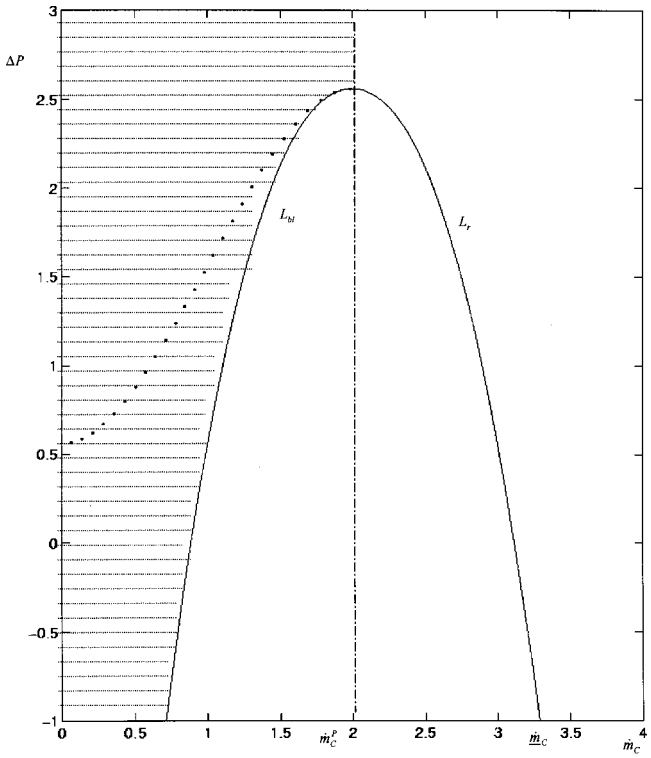

Fig. 4 Maximal uncertainty allowed in the control design

that the reduced-order dynamics possesses desired stability performance. The final step is to construct an extra control for guaranteeing that the system state will reach the sliding surface and forcing the system state to stay near the sliding surface. The sliding surface generally needs to be deliberately selected to achieve asymptotic stability of the equilibrium on the surface. In general, there are lots of choices of sliding surface for control design. In this study, we choose a special one for the robust design. As implied by Lemma 1, the amplitude of stall wave x_1 will eventually go to zero if the mass flow $\dot{m}_C^0+x_2>\dot{m}_C^P$. That means the rotating stall can be prevented and/or recovered by making $\dot{m}_C^0+x_2>\dot{m}_C^P$ for a given unstalled operating point $x^0=[0,\dot{m}_C^0,\Delta P^0]^T$. Thus, as motivated by the result of Lemma 1, the sliding surface for the robust stabilization is selected as:

$$S(x)=x_2=0. \tag{8}$$

If the system operates under the case of which $\gamma_c\leqslant\gamma\leqslant\gamma_s$, the objective of the control algorithm is to enlarge the domain of attraction of the working unstalled equilibrium x^0. In such cases, the control input $u_2(t)$ can be simply set to zero since the unstalled operating equilibrium is known to be asymptotically stable. However, when the system operates with $\gamma\leqslant\gamma_c$ due to some uncertainty on the throttle function, the control input u_2 will be used to fulfill the task of stall recovery. That is, $u_2(t)$ will be selected as a constant bias such that $\gamma+u_2=\gamma_d$, of which γ_d satisfies the relation: $\dot{m}_C^0=F(\gamma_d,\Delta P^0)$, and let the unstalled equilibrium x^0 be the desired operating point for stall recovery from rotating stall.

Now, we show the asymptotic stability of the reduced-order dynamics on the sliding surface S in Eq. (8). When the system state is trapped in the sliding surface on $S(x)=0$, the following two conditions are required to be satisfied [11]:

$$S=0 \quad \text{and} \quad \dot{S}=0. \tag{9}$$

The reduced dynamics on the sliding surface is then obtained from Eqs. (4) and (6), by letting $x_2=0$, as

$$\frac{dx_1}{dt}=\frac{\alpha}{\pi W}\int_0^{2\pi} C_{ss}(\dot{m}_C^0+Wx_1\sin\theta)\sin\theta\, d\theta, \tag{10}$$

$$\frac{dx_3}{dt}=\frac{1}{4B^2}\{\dot{m}_C^0-F(\gamma^0+u_2(t),x_3+\Delta P^0)\}. \tag{11}$$

For simplicity, choose the Lyapunov function candidate

$$V(x_1,x_3)=\frac{1}{2}\cdot(x_1^2+4B^2x_3^2). \tag{12}$$

for the reduced dynamics (10)–(11). Taking the time derivative of $V(x_1,x_3)$ along the trajectory of the reduced model (10)–(11), we have

$$\begin{aligned}\dot{V}(x_1,x_3)&=x_1\dot{x}_1+x_3\{\dot{m}_C^0-F(\gamma^0+u_2(t),\Delta P^0+x_3)\}\\&=x_3\cdot\{F(\gamma_d,\Delta P^0)-F(\gamma_d,\Delta P^0+x_3)\}+x_1\dot{x}_1.\end{aligned} \tag{13}$$

Since $F(\gamma,\Delta P)$ is assumed to be strictly increasing with respect to both γ and ΔP, it follows that $x_3\cdot\{F(\gamma_d,\Delta P^0)-F(\gamma_d,\Delta P^0+x_3)\}\leqslant 0$ and the equality holds only at $x_3=0$. Therefore, by Lemma 1, we have $-\dot{V}(x_1,x_3)$ is a (locally) positive definite function for $\dot{m}_C^0>\dot{m}_C^P$. This implies that the asymptotic stability of the unstalled equilibrium x^0 is provided on the sliding surface $S=0$.

Next, we propose a control law to guarantee the reaching condition for a prescribed region Ω in the state space. That is, the domain of attraction of the operating equilibrium will be enlarged with a certain extent. To give a clear definition of the subspace Ω, a real value $B_l<\dot{m}_C^P$ is assumed to satisfy the following condition:

$$C_{ss}(\dot{m}_C)\leqslant C_{ss}(\dot{m}_C^P) \quad \text{for all} \quad \dot{m}_C\geqslant B_l. \tag{14}$$

In fact, B_l can always be found from conditions (H1) and (H2). It is clear that a positive constant $M_l\leqslant\dot{m}_C^0-B_l/W$ exists since $\dot{m}_C^0>\dot{m}_C^P>B_l$. For the proof of reaching condition, the subset Ω is defined as:

$$\Omega:=\{x\in R^3\,\|x_1|\leqslant M_l, x_2\geqslant B_l-\dot{m}_C^0+WM_l\}. \tag{15}$$

Apparently, M_l is the allowed upper bound for the state variable $A(t)$ to deviate from its equilibrium value; while $B_l-\dot{m}_C^0+WM_l$ is that for the state variable $\dot{m}_C(t)$. The size of Ω depends on the choice of M_l and B_l. In practical applications, the value of B_l is first decided to be as small as possible from the nominal $C_{ss}(\cdot)$ function. The value of M_l is then decided from the inequality: $B_l-\dot{m}_C^0+WM_l<0$. By the definition of Ω as in Eq. (15), we have $x_2+\dot{m}_C^0+Wx_1\sin\theta\geqslant B_l+WM_l-Wx_1\geqslant B_l$. It then follows from Eq. (14) that

$$C_{ss}(x_2+\dot{m}_C^0+Wx_1\sin\theta)\leqslant C_{ss}(\dot{m}_C^P), \quad \text{for all } 0\leqslant\theta\leqslant 2\pi \text{ and } x\in\Omega. \tag{16}$$

The inequality (16) above can be regarded as the key property that characterizes all the states within the set Ω.

We now show the reaching property for the sliding surface S by using the Lyapunov criterion. Choose the Lyapunov function candidate as

$$V(S):=\frac{1}{2}S^2. \tag{17}$$

Taking the time derivative of $V(S)$ along the trajectories of system (4)–(6), we have

$$\dot{V}(S)=S\dot{S}=x_2\dot{x}_2=-x_3x_2-(\Delta P^0)x_2+\frac{x_2}{2\pi}\times\int_0^{2\pi}C_{ss}(x_2+\dot{m}_C^0+Wx_1\sin\theta)d\theta+x_2\cdot u_1. \quad (18)$$

To assure $\dot{V}(S)<0$ for all trajectories with initial lying within Ω, the control law is proposed as:

$$u_1(t)=\begin{cases}x_3(t) & \text{for } x_2(t)>0,\\ x_3(t)+[C_{ss}(\dot{m}_C^0)-C_{ss}^m(t)] & \text{for } x_2(t)<0,\end{cases} \quad (19)$$

where

$$C_{ss}^m(t)=\begin{cases}0 & \text{when } x_2(t)+\dot{m}_C^0+Wx_1(t)\leq\dot{m}_C,\\ C_{ss}(x_2(t)+\dot{m}_C^0+Wx_1(t)) & \text{when } x_2(t)+\dot{m}_C^0+Wx_1(t)>\dot{m}_C.\end{cases} \quad (20)$$

Note that, $C_{ss}^m(t)$ defined in Eq. (20) is obtainable from the stable branch of the function $C_{ss}(\cdot)$, which is measurable. The reaching condition is hence provided by the next lemma.

Lemma 2. Suppose $C_{ss}(\dot{m}_C)$ satisfies Hypothesis 1. Then the reaching condition for system (4)–(6) is guaranteed by the control u_1 as in (19) for all initials lying within Ω, where Ω is given in (15).

Proof: see Appendix A.

Remark 2. As discussed previously, there exists no constraint on x_3 for reaching condition. In addition, by Lemma 1 and previous discussions, the stability of the reduced dynamics on $S=0$ is provided for all $x=(x_1,x_2,x_3)^T$ with $\dot{m}_C^0+x_2>\dot{m}_C^P$. According to the principle of SMC design, the DOA of the unstalled equilibrium x^0 is hence governed only by Ω, as in (15).

The next theorem follows readily from Lemma 2 and the stability on the sliding surface.

Theorem 1. Suppose $C_{ss}(\cdot)$ satisfies Hypothesis 1. Then the domain of attraction of the unstalled equilibrium x^0 for system (4)–(6) can be enlarged to the extent of Ω as defined in (15). The proposed control design is robust with respect to the uncertainties in the function $C_{ss}(\cdot)$.

The control u_1 defined in Eq. (19) for $x_2(t)>0$ is mainly used for cancellation. As given in the next lemma, such control force can be set to zero.

Lemma 3. Suppose the state trajectory of system (4)–(6) can be constrained within the half space $\Psi:=\{x|x_2+\dot{m}_C^0>\dot{m}_C^P\}$ by a suitable control. Then it will eventually converge to the equilibrium point x^0.

Proof: Let the Lyapunov function candidate be given by

$$V(x_1,x_2,x_3)=\frac{1}{2}(x_1^2+x_2^2+4B^2x_3^2).$$

Then the time derivative of V along the system trajectory of system (4)–(6) for $x_2(t)>0$ yields

$$\begin{aligned}\dot{V}(x_1,x_2,x_3)|_{x_2(t)>0}&=x_1\dot{x}_1+x_2\dot{x}_2+4B^2x_3\dot{x}_3\\ &\leq x_2\dot{x}_2+4B^2x_3\dot{x}_3 \quad \text{(By Lemma 1)}\\ &=-x_2x_3+\frac{x_2}{2\pi}\int_0^{2\pi}[C_{ss}(x_2+\dot{m}_C^0\\ &\quad +Wx_1\sin\theta)-C_{ss}(\dot{m}_C^0)]d\theta+4B^2x_3\dot{x}_3\end{aligned}$$

In the derivation above, u_1 is set to zero for $x_2>0$. This leads to that $x_2/2\pi\int_0^{2\pi}[C_{ss}(x_2+\dot{m}_C^0+Wx_1\sin\theta)-C_{ss}(\dot{m}_C^0)]d\theta<0$ for $x_2>0$. As implied by the proof of Lemma 2, we have

$$\begin{aligned}\dot{V}(x_1,x_2,x_3)|_{x_2(t)>0}&\leq-x_2x_3+(\dot{m}_C^0)x_3+x_2x_3-x_3F(\gamma,\Delta P^0+x_3)\\ &=x_3\{F(\gamma,\Delta P^0+x_3)-F(\gamma,\Delta P^0)\}\leq 0,\end{aligned}$$

where the equality holds only when $x=0$. Q.E.D.

To smooth the chattering behaviors, a boundary layer of $-\delta<x_2<\delta$ is introduced. The control law is modified as:

$$u_1(t)=\begin{cases}x_3(t) & \text{when } x_2(t)>\delta,\\ x_3(t)-k_2(t)(x_2+\delta) & \text{when} -\delta\leq x_2(t)\leq\delta,\\ x_3(t)+[C_{ss}(\dot{m}_C^0)-C_{ss}^m(t)] & \text{when } x_2(t)<-\delta.\end{cases} \quad (21)$$

Here $C_{ss}^m(t)$ is given as in (20) and $k_2(t)=C_{ss}(\dot{m}_C^0)-C_{ss}^m(t)/2\delta$. It is not difficult to check that the practical stability of the closed-loop system (4)–(6) is guaranteed by the control u_1 as in Eq. (21). As implied by Lemma 3, $u_1(t)$ can also be set to zero for $x_2(t)>0$ to save the control effort.

4 Numerical Results

In the following, the proposed control laws proposed in Section 3 are applied to a specific compression system to demonstrate the validity of the main design.

Consider the system of (1)–(3) with $C_{ss}(\cdot)$ adopted from [3] as given by:

$$C_{ss}(y)=-0.5(y-1)^3+1.5(y-1)+1.56. \quad (22)$$

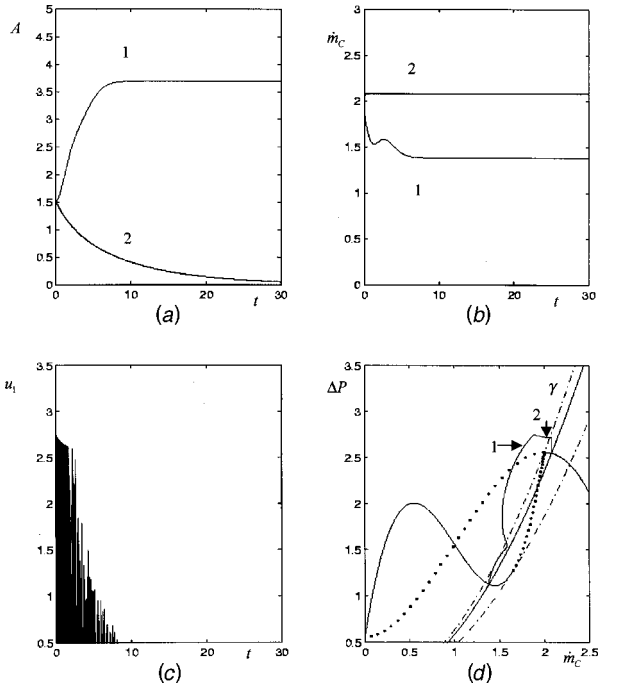

Fig. 5 Results for operation in the pre-stalled zone (*a*) A versus t, (*b*) mass flow versus t, (*c*) versus t, (*d*) plot in the phase plane

The system parameters and control for the numerical study are selected and calculated as $\alpha=0.4114$; $W=0.3$; $B=0.4$; $\dot{m}_C^P=2.0$; $\dot{m}_C^0=2.08$; $\underline{\dot{m}}_C\approx 3.15$; $\delta=0.05$; $k_2=25.5$. In addition, B_l is chosen to be -1.0, which can be justified from Eq. (22). Moreover, M_l can be selected to 10.0 from the discussions in Section 3.2. However, to allow a larger deviation of $\dot{m}_C^0$, M_l is set to 3.0, which is large enough for practical considerations.

From Eq. (21), the control input u_1 can then be obtained

$$u_1(t)=\begin{cases} x_3 & \text{when } x_2>0.05, \\ x_3-k_2(x_2+0.05) & \text{when } -0.05\leqslant x_2\leqslant 0.05, \\ x_3+C_{ss}(2.08) & \text{when } -2.18<x_2<-0.05 \\ & \text{and } \dot{m}_C(t)+0.3x_1(t)\leqslant 3.15 \\ x_3+C_{ss}(2.08)+C_{ss}(\dot{m}_C(t)+0.3x_1(t)) & \text{when } -2.18<x_2<-0.05 \\ & \text{and } \dot{m}_C(t)+0.3x_1(t)>3.15 \end{cases} \tag{23}$$

Case 1. Behavior of Nominal System. Let $\gamma^0=1.3$. As depicted by trajectory 2 in Fig. 2, the system might run into rotating stall under large disturbances since $\gamma_c\leqslant\gamma^0\leqslant\gamma_s$. The control force defined in Eq. (24) is now utilized to force the system back to the desired unstalled equilibrium x^0. The DOA of x^0 in Eq. (15) can then be obtained as:

$$\Omega:=\{x|0\leqslant x_1\leqslant 3.0,\ x_2\geqslant -2.18\}. \tag{24}$$

Numerical results for the control system are shown in Fig. 5. The time responses without and with control with initial $x^0=[1.5,1.88,2.769]^T$ are depicted in trajectories 1 and 2, respectively. Since a great extent of uncertainty in the compressor characteristic is allowed for the proposed designs, as depicted in Fig. 5(*c*), a large control force guaranteeing the system state to reach the sliding surface is expected. When the transient is forced to be within the boundary layer, the control is switched to the linear state feedback and therefore the control force is dramatically reduced as observed in Fig. 5 for $t>0.5$. The transient state is forced back to x^0 as depicted by trajectory 2 in Fig. 5(*d*).

Case 2. Behavior of Perturbed System. Next, we approximate the $C_{ss}(\cdot)$ in Eq. (22) by:

$$\tilde{C}_{ss}(\dot{m}_C)=-0.4722\dot{m}_C^3+1.3069\dot{m}_C^2+0.3174\dot{m}_C+0.5039. \tag{25}$$

For clarity, compressor characteristics as defined by (22) and (25) are redrawn in Fig. 6. Note that small deviations exist between the two functions. One can treat Eq. (22) as the nominal model and Eq. (25) as a perturbed one. To justify the robustness of the control designs, the same initial and target states in Fig. 5 are used again while the $C_{ss}(\cdot)$ function in Eq. (22) is now replaced by Eq. (25) for numerical study. In this case we use the same control laws as in (23). The numerical results are shown in Fig. 7. It is observed that the performance is not influenced by the uncertainty embedded in the variation of the $C_{ss}(\cdot)$ function. However, again, the price of a large control force must be paid for, as depicted in

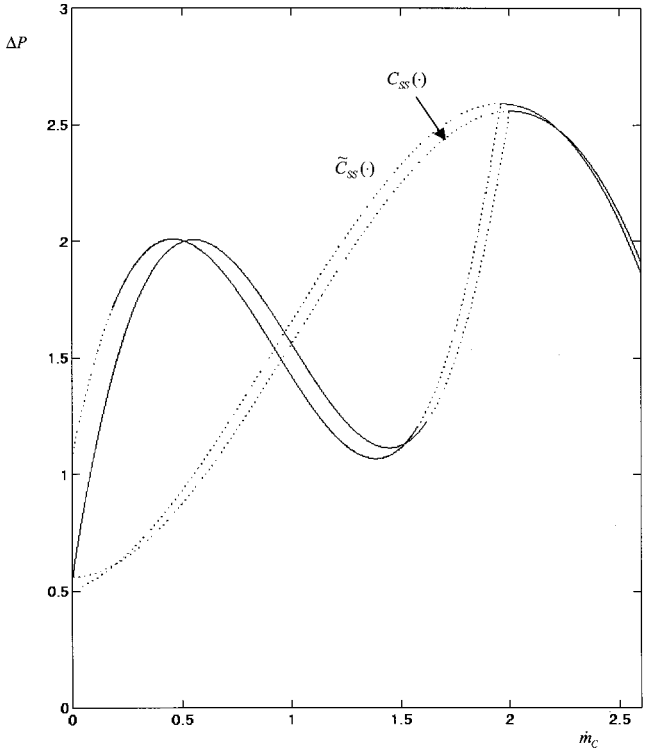

Fig. 6 Two compressor characteristics used in the simulation works

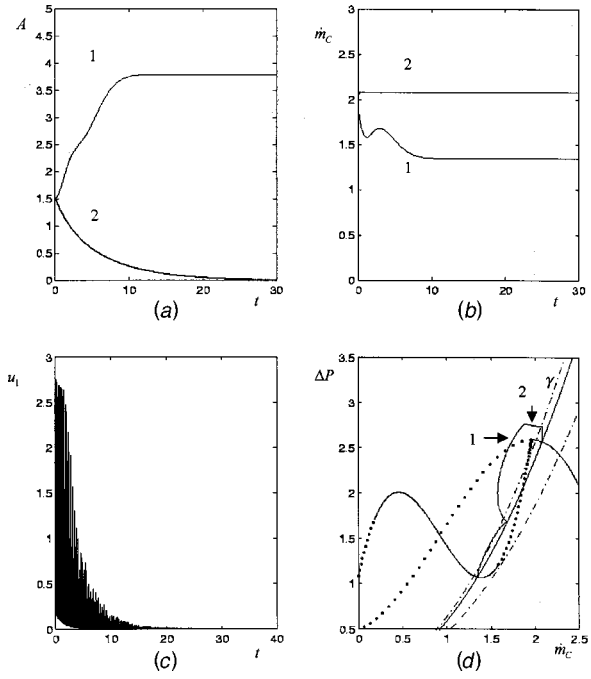

Fig. 7 Results of Case 2 for operation in the pre-stalled zone (*a*) A versus t, (*b*) mass flow versus t, (*c*) u versus t, (*d*) plot in the phase plane

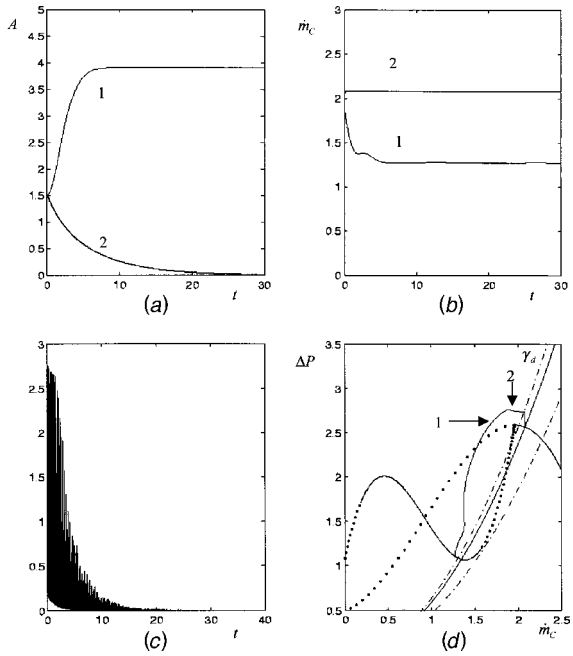

Fig. 8 Results of Case 2 for operation in the stalled zone (*a*) A versus t, (*b*) mass flow versus t, (*c*) u versus t, (*d*) plot in the phase plane

Fig. 7(*c*). For the operations with $\gamma \leqslant \gamma_c$, the results for stall recovery given in Fig. 8 are also quite satisfactory. In this case, $\gamma = 1.22 < \gamma_c = 1.25$ and u_2 is set to 0.08 as a constant bias such that $\gamma + u_2 = \gamma_d = 1.3$. The new value γ_d provides a desired unstalled equilibrium.

5 Conclusions

By utilizing an additive-type actuation for the mass flow dynamics, the DOA of the unstalled equilibria has been enlarged via sliding mode control designs. The design was shown to be robust with respect to the uncertainty embedded in the unstable portion of the axisymmetric compressor characteristic. The robust design mainly depends on the knowledge of the stable portion of compressor characteristic, which is usually measurable by deliberate experiments. Though large control effort might be required, the proposed study is surely attractive in real applications. In fact, the amount of control efforts is mainly dependent on the magnitude of system uncertainties and/or disturbance.

Acknowledgments

The authors are grateful to the reviewers for their comments and suggestions. This research was supported by the Nation Science Council, Taiwan, ROC under Grants NSC 87-2212-E-009-040, NSC 88-2212-E-009-020 and NSC 88-2212-E-009-021.

Appendix A

A proof of Lemma 2 is given as follows.

Proof: Substituting Eq. (19) into the right-hand side of Eq. (18) yields

$$S\dot{S} = x_2\dot{x}_2 = \begin{cases} \dfrac{x_2}{2\pi}\displaystyle\int_0^{2\pi} C_{ss}(x_2 + \dot{m}_C^0 + Wx_1 \sin\theta)d\theta - x_2 \cdot (\Delta P^0), & \text{for } x_2 > 0 \\ \dfrac{x_2}{2\pi}\displaystyle\int_0^{2} [C_{ss}(x_2 + \dot{m}_C^0 + Wx_1 \sin\theta) - C_{ss}^m(t)]d\theta, & \text{for } x_2 < 0. \end{cases} \tag{26}$$

The objective of the control design is to assure $S\dot{S} < 0$ for all state trajectories with initials lying within Ω and $x_2 \neq 0$. First, consider the case of which $x_2 > 0$. Two subcases listed below are separately studied:

(C1) $x_2(t) + \dot{m}_C^0 - Wx_1(t) \geqslant \dot{m}_C^P$,
(C2) $x_2(t) + \dot{m}_C^0 - Wx_1(t) < \dot{m}_C^P$.

As pointed out in Section 3.1, from (H2) $C_{ss}(\cdot)$ is a concave function in the region $J := \{\dot{m}_C | \dot{m}_C \geqslant \dot{m}_C^P\}$. Thus, for case (C1) we have

$$\begin{aligned} S\dot{S} &= \frac{x_2}{2\pi}\int_0^{2\pi} [C_{ss}(x_2 + \dot{m}_C^0 + Wx_1 \sin\theta) - C_{ss}(\dot{m}_C^0)]d\theta \\ &< \frac{x_2}{2\pi}\int_0^{2\pi} [C_{ss}(x_2 + \dot{m}_C^0 + Wx_1 \sin\theta) \\ &\quad - C_{ss}(x_2 + \dot{m}_C^0)]d\theta \quad (\text{by (H2)}) \\ &\leqslant \frac{x_2}{2\pi}\int_0^{2\pi} C_{ss}'(x_2 + \dot{m}_C^0) \cdot Wx_1 \sin\theta d\theta \quad (\text{by concavity}) = 0. \end{aligned} \tag{27}$$

For case (C2), since $x_2(t) + \dot{m}_C^0 > \dot{m}_C^P$ and $x_2(t) + \dot{m}_C^0 - Wx_1(t) < \dot{m}_C^P$, it follows that $-1 < \dot{m}_C^P - x_2(t) - \dot{m}_C^0/Wx_1(t) < 0$. Let $\theta_t = \sin^{-1}(\dot{m}_C^P - x_2(t) - \dot{m}_C^0/Wx_1(t))$. Then θ_t exists and $\theta_t < 0$. Since $C_{ss}(\cdot)$ is a concave function, by Definition 1, we have

$$\begin{aligned} &C_{ss}(x_2 + \dot{m}_C^0 + Wx_1 \sin\theta) \\ &\quad \leqslant C_{ss}(x_2 + \dot{m}_C^0) + C_{ss}'(x_2 + \dot{m}_C^0) \cdot Wx_1 \sin\theta, \\ &\qquad \text{for all } 0 \leqslant \theta \leqslant \pi - \theta_t \text{ and } 2\pi + \theta_t \leqslant \theta \leqslant 2\pi. \end{aligned} \tag{28}$$

Similarly, from Eq. (16) and the concavity of $C_{ss}(\cdot)$ we have

$$\begin{aligned} &C_{ss}(x_2 + \dot{m}_C^0 + Wx_1 \sin\theta) \\ &\quad \leqslant C_{ss}(\dot{m}_C^P), \\ &\quad \leqslant C_{ss}(x_2 + \dot{m}_C^0) + C_{ss}'(x_2 + \dot{m}_C^0) \cdot (\dot{m}_C^P - x_2(t) - \dot{m}_C^0) \\ &\quad = C_{ss}(x_2 + \dot{m}_C^0) + C_{ss}'(x_2 + \dot{m}_C^0) \cdot Wx_1 \sin\theta_t \\ &\quad \leqslant C_{ss}(x_2 + \dot{m}_C^0) + C_{ss}'(x_2 + \dot{m}_C^0) \cdot Wx_1 \sin\theta \\ &\qquad \text{for all } \pi - \theta_t < \theta < 2\pi + \theta_t. \end{aligned} \tag{29}$$

Thus, for case (C2) it is clear that

$$S\dot{S} = \frac{x_2}{2\pi}\int_0^{2\pi}[C_{ss}(x_2+\dot{m}_C^0+Wx_1\sin\theta)-C_{ss}(\dot{m}_C^0)]d\theta$$

$$< \frac{x_2}{2\pi}\int_0^{2\pi}[C_{ss}(x_2+\dot{m}_C^0+Wx_1\sin\theta)-C_{ss}(x_2+\dot{m}_C^0)]d\theta$$

$$\leqslant \frac{x_2}{2\pi}\int_0^{2\pi}C'_{ss}(x_2+\dot{m}_C^0)\cdot Wx_1\sin\theta d\theta = 0 \qquad (30)$$

Thus, by Eq. (30) and Lemma 1, the state trajectory will never leave the set Ω and approach to the sliding surface S eventually for all initials lying within Ω with $x_2(0)>0$.

Next, we consider the case of which $x_2<0$. Similarly, two subcases are studied separately:

(C3) $x_2(t)+\dot{m}_C^0+Wx_1(t)\leqslant \underline{\dot{m}}_C$
(C4) $x_2(t)+\dot{m}_C^0+Wx_1(t)>\underline{\dot{m}}_C$.

For case (C3), we have $C_{ss}^m=0$ and

$$S\dot{S} = \frac{x_2}{2\pi}\int_0^{2\pi}C_{ss}(\dot{m}_C^0+x_2+Wx_1\sin\theta)d\theta<0. \quad \text{(by (H3))}$$

For case (C4), we have $C_{ss}^m(t)=C_{ss}(x_2(t)+\dot{m}_C^0+Wx_1(t))<0$. Denote $\theta_1=\sin^{-1}(x_2(t)+\dot{m}_C^0-\underline{\dot{m}}_C/Wx_1(t))$. It is clear that θ_1 is solvable. We then have

$$S\dot{S} = \frac{x_2}{2\pi}\int_0^{\pi+\theta_1}[C_{ss}(\dot{m}_C^0+x_2+Wx_1\sin\theta)-C_{ss}^m(t)]d\theta$$

$$+\frac{x_2}{2\pi}\int_{\pi+\theta_1}^{2\pi+\theta_1}[C_{ss}(\dot{m}_C^0+x_2+Wx_1\sin\theta)-C_{ss}^m(t)]d\theta$$

$$+\frac{x_2}{2\pi}\int_{2\pi+\theta_1}^{2\pi}[C_{ss}(\dot{m}_C^0+x_2+Wx_1\sin\theta)-C_{ss}^m(t)]d\theta$$

$$<\frac{x_2}{2\pi}\int_{\pi+\theta_1}^{2\pi+\theta_1}[C_{ss}(\dot{m}_C^0+x_2+Wx_1\sin\theta)-C_{ss}(x_2(t)+\dot{m}_C^0$$

$$+Wx_1(t))]d\theta<0$$

Based on the discussions above, the final condition is thus proved. Q.E.D.

Nomenclature

A = amplitude of the first angular mode of rotating wave
ΔP= nondimensional pressure rise within the plenum
$\dot{m}_C$= nondimensional compressor mass flow rate
θ = circumferential coordinate
B = Greitzer B-parameter, proportional to rotor speed
α = a geometry-related constant
W = scaling parameter for normalized velocities
C_{ss}= nondimensional axisymmetric compressor characteristic
C'_{ss}= first derivative of C_{ss} function
C''_{ss}= second derivative of C_{ss} function
F = nondimensional throttle function
γ = control parameter of throttle function

References

[1] Kerrebrock, J. L., 1990, *Aircraft Engines and Gas Turbines*, 2nd Ed., MIT Press.
[2] Paduano, J. D., Epstein, A. H., Valavani, L., Longley, J. P., Greitzer, E. M., and Guenette, G. R., 1993, ''Active Control of Rotating Stall In a Low Speed Axial Compressor,'' ASME J. Turbomach., **115**, pp. 45–56.
[3] Liaw, D.-C., and Abed, E. H., 1996, ''Active Control of Compressor Stall Inception: a Bifurcation-Theoretic Approach,'' Automatica , **32**, pp. 109–115.
[4] Krstić, M., Protz, J. M., Paduano, J. D., and Kokotović, P. V., 1995, ''Backstepping Designs for Jet Engine Stall and Surge Control,'' Proceedings of the 34th IEEE Conference on Decision and Control. pp. 3049–3055.
[5] Moore, F. K., and Greitzer, E. M., 1986, ''A Theory of Post-Stall Transients in Axial Compression Systems: Part I-Development of Equations,'' ASME J. Eng. Gas Turbines Power, **108**, pp. 68–76.
[6] Badmus, O. O., Chowdhury, S., Eveker, K. M., Nett, C. N., and Rivera, C. J., 1995, ''Simplified approach for control of rotating stall, Part I,'' J. Propul. Power, **11**, pp. 1195–1209.
[7] Badmus, O. O., Chowdhury, S., Eveker, K. M., Nett, C. N., and Rivera, C. J., 1995, ''Simplified approach for control of rotating stall, Part II,'' J. Propul. Power, **11**, pp. 1210–1223.
[8] Liaw, D.-C., and Huang, J.-T., 1998, ''Global Stabilization of Axial Compressors Using Nonlinear Cancellation and Backstepping Designs,'' Int. J. Syst. Sci., **29**, pp. 1345–1361.
[9] Paduano, J. D., Valavani, L., and Epstein, A. H., 1993, ''Parameter Identification of Compressor Dynamics during Closed-Loop Operation,'' ASME J. Dyn. Syst., Meas., Control, **115**, pp. 694–703.
[10] Haddad, W. M., Fausz, J. L., Chellaboina, V., and Leonessa, A., 1997, ''Nonlinear Robust Disturbance Rejection Controllers for Rotating Stall and Surge in Axial Flow Compressors,'' Proceedings of the IEEE Conference on Control Applications, pp. 767–772.
[11] Utkin, V. I., 1987, ''Discontinuous Control System: State of Art in Theory and Application,'' 10th IFAC on Automation Control, Vol. 1, pp. 1782–1786.
[12] Simon, J. S., and Valavani, L., 1991, ''A Lyapunov Based Nonlinear Control Scheme for Stabilizing a Basic Compression System Using a Close-Coupled Control Valve,'' Proceedings of the 1991 American Control Conference, pp. 2398–2406.
[13] Hendricks, G. J., and Gysling, D. L., 1994, ''Theoretical study of sensor-actuator schemes for rotating stall control,'' J. Propul. Power, **10**, pp. 101–109.
[14] Doedel, E. J., 1981, AUTO: A Program for the Automatic Bifurcation Analysis of Autonomous Systems. Congressus Numerantium, **30**, pp. 265–284.
[15] McCaughan, F. E., 1989, ''Application of Bifurcation Theory to Axial Flow Compressor Instability,'' ASME J. Turbomach., **111**, pp. 426–433.
[16] Harris, L. P., and Spang, H. A., 1991, ''Compressor Modeling and Active Control of Stall/Surge,'' Proc. 1991 American Control Conference, pp. 2392–2397.
[17] DeCarlo, R. A., Zak, S. H., and Matthews, G. P., 1988, ''Variable Structure Control of Nonlinear Multivariable System: A Tutorial,'' Proceedings of the IEEE, **76**, pp. 212–232.
[18] Slotine, J.-J. E., and Ji, W., 1991, *Applied Nonlinear Control*, Prentice-Hall, New Jersey.